Proc. 1997 IEEE-Ultrasonics Symposium, to be published

Ultrasonic Reflection Tomography and Tomographic Parameter Extraction for Post-Discotomic Scarring Diagnostics

A. Pesavento[1], H. Ermert[1], E. Broll Zeitvogel[2] and J. Grifka[2]
[1]Dept. of Electrical Engineering, Ruhr University, Bochum, Germany
[2]St. Joseph University Hospital, Bochum, Germany

Abstract - An ultrasonic imaging system is presented for diagnostics of post discotomic scarring. The system consists of a conventional B-mode imaging system, using a 5 MHz sector scanner. The scanner is laterally moved over the patients back along a linear line. Thus several images of the same cross sectional plane are acquired by sampling the RF echo data. This data has been used for both, spatial compounding of the B-mode images and multidirectional extraction of the spectral parameters attenuation and backscattering.

INTRODUCTION

Up to 40% of all back surgery patients suffer from significant post-operative relapsing complaints frequently caused by scarring. Despite modern X-ray and MR imaging systems there is still a lack of a reliable screening diagnostics. The image quality of conventional B-scans suffers from low contrast and shadows. Medical aims of screening are detection and evaluation of scares and measurement of muscle volumina. In the past the ultrasound image quality of organs which allow multidirectional scanning like breast, thyroid, and testicles was improved significantly by tomographic concepts such as ultrasonic reflection tomography. In this concept, B-mode images of the same cross sectional plane but from different aspect directions (subimages) are acquired and added incoherently. A conventional sector scanner is moved mechanically in lateral direction over the patients back (Figure 1). Averaging of the subimages significantly reduces speckle. The acquired multidirectional RF echo data can further be used for a multidirectional extraction of physical parameters, like attenuation and frequency dependent backscattering. These parameters supply additional information for the detection of scares and for the differentiation and segmentation of the tissue types in the human back. A major problem in the analysis of attenuation from echo data is the requirement of a known or homogeneous backscattering of the tissue, which is not valid for the different tissues in the human back. In order to reduce the artifacts of the attenuation estimation due to the inhomogeneity of the backscattering a special multidirectional approach has been developed that uses data from different directions.

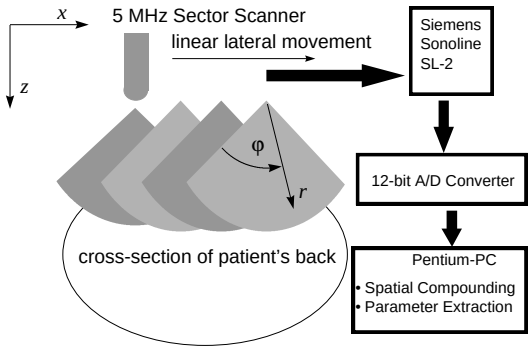

Figure 1: System setup

DATA ACQUISITION

Figure 1 shows the acquisition system. The data is acquired by a conventional single element 5 MHz sector scanner which is moved laterally by a stepper motor. A 12-bit A/D Converter samples the signal without time gain compensation.

SPATIAL COMPOUNDING

After demodulation the single images are averaged incoherently. Averaging of the single images is known to improve the image-SNR, which is 1.91 for

a single image with fully developed speckle. If N uncorrelated images are compounded, the SNR can be improved by a factor of $\sqrt{N}$. The speckle correlation of two images depends on the transducer characteristics [5], depth [1] and displacement [5]. Thus, the real speckle correlation for the given transducer was measured and the displacement of the subimages was optimized with respect to the SNR improvement [1]. This way the SNR of a homogeneously backscattering phantom was improved by 12 dB.

SPECTRUM ANALYSIS

Tissue parameters like frequency dependent attenuation and frequency dependent backscattering are derived from the power spectrum of the echo data. In this work the power spectrum $R_{uu}(\omega,\varphi_i,r_j)$ in a short segment denoted by (i,j) was estimated using periodograms. The logarithmic power spectrum in this work is defined by $L_{uu}(\omega,\varphi_i,r_j)=10\ \mathrm{dB}\ \log_{10}R_{uu}(\omega,\varphi_i,r_j)$. The segments are sectors like the B-mode images of the system. Diffraction characteristics derived from echo data of a homogeneous speckle phantom in multiple depths and the point spread function in the transducer focus were removed from the logarithmic spectra [3].

BACKSCATTER ESTIMATION

The influence of the frequency dependent global attenuation (the mean value of the attenuation for a entire image) was estimated using the Multi-Narrowband-Method (MNB) [3].

$$[\hat{\alpha}(\omega), \hat{L}_0] = \arg\min\left\{\left\| L_{uu}(\omega,\varphi_i,r_j) - \left[L_0 - \alpha(\omega) r_j\right]\right\|^2\right\}$$

The power spectra were corrected using the estimated attenuation $\hat{\alpha}(\omega)$ and intercept values $\hat{L}_0$. The corrected power spectra corresponding to different transducer positions were averaged. Only frequencies within the transducers bandwidth are considered. This way compounded frequency dependent backscattering images $b(\omega,x_i,z_i)$ are obtained. Cartesian coordinates (x_i, z_i) are introduced to consider the different geometry of the compound data.

Conventional estimation of the frequency dependent backscattering using single images requires certain segment size in order to limit the variance of the power spectrum estimator. This size can now be reduced by the number of subimages, which results in a better resolution of the backscattering estimation. Finally, a linear regression is applied to the frequency dependence of the $b(\omega,x_i,z_i)$:

$$b(\mathrm{w}, x_i, z_j) = \hat{b}_1(x_i, z_j)(\mathrm{w} - \mathrm{w}_m) + \hat{b}_m(x_i, z_j)$$

Slope $\hat{b}_1(x_i, z_j)$ and mean $\hat{b}_m(x_i, z_j)$ are displayed in parametric images.

ATTENUATION ESTIMATION

Many algorithms have been developed that successfully estimate attenuation using large image areas of homogeneously backscattering media. These algorithms work well even in case of weak backscattering inhomogeneities. To obtain quantitative attenuation images the algorithms have to be applied to a small echo data set. If backscattering is strongly inhomogeneous the following problem occurs: A single frequency component of the power spectrum L_{uu} of a single A-scan as a function of the depth r is presented schematically in Figure 2 (solid curve). The dotted lines represent linear regressions of short sections. In the MNB method the slopes of the linear regression lines estimate the local attenuation. The slope of the regression lines denoted by "1" and "2" is determined by a significant change of backscattering instead of attenuation properties. Consequently, a strong artifact occurs in the corresponding sections.

Although other methods than MNB can be applied and lateral averaging can reduce this effect the described artifact is the major problem for algorithms, which estimate the local attenuation.

Our new multidirectional approach uses a different strategy to avoid this problem. As shown in Figure 2 (left image) a strongly attenuating region will present a shadow. This shadow will change its position with the direction of insonification. This can be exploited to estimate the attenuation in a more robust way:

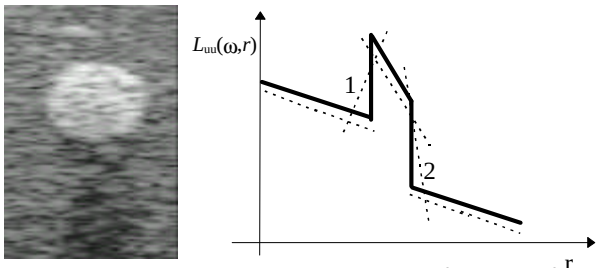

Figure 2: schematic power spectrum at a single frequency of a A-scan through a phantom

1. The global attenuation at each frequency (MNB-method) is estimated and the spectra are corrected as described in preceding section.
2. The lateral mean value of the log spectra

$$\overline{L}_{uu}(\omega, r_j) = \frac{1}{N}\sum_{i=1}^{N} L_{uu}(\omega, \varphi_i, r_j)$$

is calculated and removed from the data in order to avoid artifacts due to the layered structure of the back.

3. The local mean value m and center of gravity s for each pixel (i,j) are defined by:

$$m(i,j,n) = \frac{\sum_{k=i-n}^{k=i+n} L_{uu}(\omega, \varphi_j, r_k) \cdot o\left(L_{uu}(\omega, \varphi_j, r_k)\right)}{\sum_{k=1}^{k=1+n} o\left(L_{uu}(\omega, \varphi_j, r_k)\right)}$$

$$s(i,j,n) = \frac{\sum_{k=i-n}^{k=i+n} x_j \cdot o\left(L_{uu}(\omega, \varphi_j, r_k)\right)}{\sum_{k=1-n}^{k=1+n} o\left(L_{uu}(\omega, \varphi_j, r_k)\right)}$$

$$o(L) = 1 \quad \text{if } |L| < \text{threshhold},\ 0 \quad \text{otherwise}$$

Those values of L_{uu} that are not within the amplitude range from -8 dB to 8 dB (caused by strong scatterers or borders) are omitted.

4. The attenuation corresponding to a certain pixel (φ_i, r_j) is finally estimated by:

$$\alpha(\omega, \varphi_i, r_j) = \frac{m(i+\Delta/2, \Delta/2) - m(i-\Delta/2, j, \Delta/2)}{s(i+\Delta/2, \Delta/2) - s(i-\Delta/2, j, \Delta/2)}$$

Δ represents a range of depth of approximately 3 cm.

Note, that the axial resolution of the estimator can not be better than Δ. The lateral resolution is the same as the lateral resolution of the B-mode images. If several of these parametric images are compounded, an axial resolution between the lateral and axial resolution of the attenuation estimator for a single image is obtained. The same is true for the lateral resolution. This way an acceptable and nearly isotropic resolution of about 5 mm is obtained.

RESULTS

Figure 3 compares conventional B-mode images with compounded images of a speckle phantom. The speckle reduction is obvious. It is about 12 dB in the center of the compounded image.

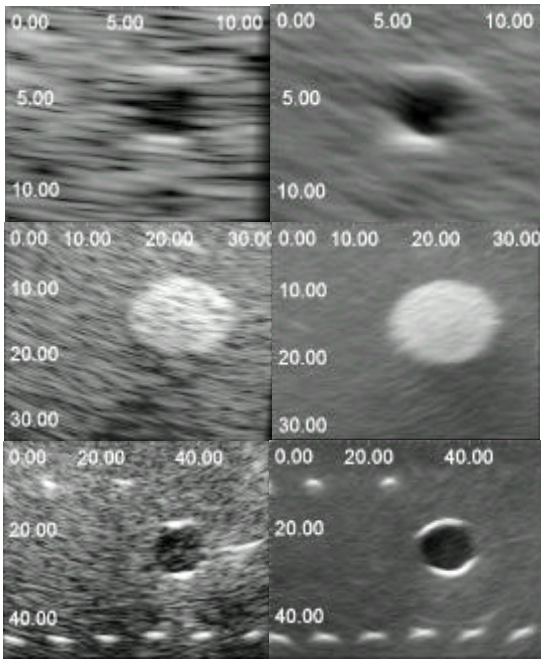

Figure 3: Comparison of single images of a speckle phantom (left) and compounded images (right). Metrics in mm. Note the different scale.

Figure 4 shows images of the back of a post-discotomy patient with scarring on the right side. In contrast to the conventional B-mode image the perturbation of the facia due to the surgery is well defined in the tomographic image (low echogenicity in region 1). The asymmetry in the echogenicity of the left and the right side of the processus spinosus with higher echogenicity on the right side indicates the scarring (region 2).

Figure 2 shows quantitative images of attenuation and the slope of the backscattering b_1 of the lower speckle phantom in Figure 3. Bright areas represent regions with low attenuation. There is an obvious correlation between low backscattering and low attenuation.

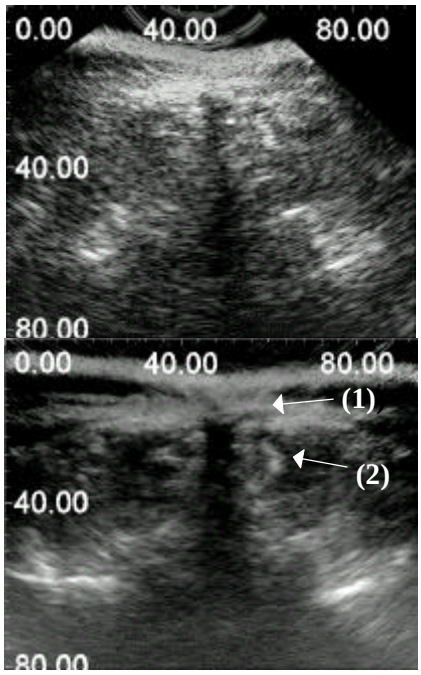

Figure 4. Comparision of in vivo images of a back of a PDS-patient. a) single image b) compounded image

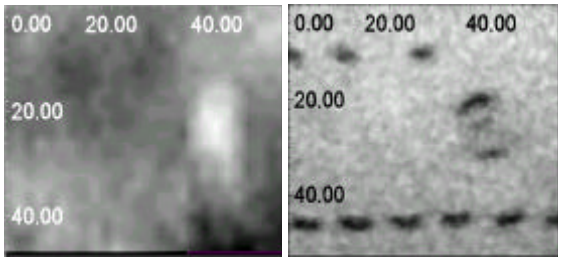

Figure 5. Attenuation image (left) and slope of backscattering (right) of the bottom image in Figure 3

On the right side, Figure 6 shows an in vivo image of the backscattering of the same data set. As expected, its information is very similar to the compounding images, which is a good estimator for the backscattering, due to the speckle reduction.

On the left side, Figure 6 shows an in vivo image of the attenuation obtained from the same echo data set, which is used for the compound image in Figure 4. It contains useful information for the segmentation of the muscle.

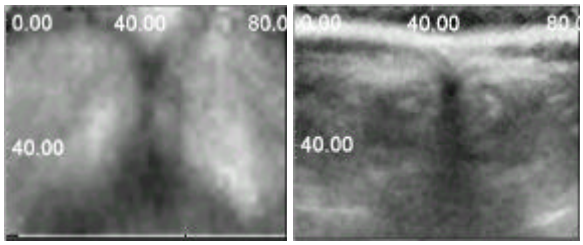

Figure 6. in vivo image of attenuation (left) and in vivo image of backscattering (right).

CONCLUSIONS

Multidirectional ultrasonic imaging enhances the diagnostics of the post-discotomy syndrom. It enables both: spatial compounding to reduce speckle considerably (12 dB) and an enhanced extraction of parameters for Tissue Characterization: Multidirectional data sets can be used for frequency dependent backscattering estimation with high spatial resolution as well as a robust estimation of frequency dependent attenuation. These parameters contain useful information for the detection of scarring and the volumetric segmentation of the muscle.

ACKNOWLEDGMENTS

This work was supported by the Deutsche Forschungsgemeinschaft, grant Gr 1506/1-1.

REFERENCES

[1] A. Pesavento, H. Ermert, J. Grifka, E. Broll-Zeitvogel, "Ultrasonic Reflection Tomography of Post-Discotomic Scarring," *Acoustical Imaging 23*, in press, New York: Plenum Press

[2] G. Schmitz, H. Ermert, T. Senge, "Color-coded tissue characterization images of the prostate," *Acoustical Imaging 22*, pp. 359-364, New York: Plenum Press, 1996

[3] Theoretical framework for spectrum analysis in ultrasonic tissue characterization, *J. Acoust. Soc. Am*, vol 73 pp. 1366-1373, 1982

[4] R. F. Wagner, M. F. Insana and S. W. Smith, "Fundamental Correlation Lengths of Coherent Speckle in Medical Ultrasonic Images," *Trans. Ultrason. Ferroelec. Freq. Contr*., vol . 35 pp34-44, 1988

[5] G. E. Trahey, S. W. Smith and O. T v. Ramm, "Speckle Pattern Correlation with Lateral Aperture Translation: Experimental Results an Implications for Spatial Compounding", *Trans. Ultrason. Ferroelec. Freq Contr*, vol. 33 pp. 257-264 ,1986

[6] M. O'Donnell and S. D. Silverstein, "Optimum Displacement for Compound Image Generation in Medical Ultrasound," *Trans. Ultrason. Ferroelec. Freq Contr.*, vol 35 pp 470-476, 1988

[7] A. Lorenz, L. Weng and H. Ermert, A Gaussian Model Approach for the Prediction of Speckle Reduction with Spatial and Frequency Compounding, *Ultrasonic Symposium*, 1996

[8] G. Röhrlein, H. Ermert, "Limited angle reflection-mode computerized tomography," *Acoustical Imaging 14*, pp. 413-424, 1986

[9] H. J. Huisman, J.M. Thijssen, "Precision and Accuracy of Acoustospectrographic Parameters", *Ultrason. Med. & Bio*., vol. 22 pp 855-871, 1996